Journal of Electrical Systems and Information Technology xxx (2016) xxx–xxx
www.elsevier.com/locate/jesit

Torque capability improvement of sensorless FOC induction machine in field weakening for propulsion purposes

Nisha G.K. [a,*], Lakaparampil Z.V. [b], Ushakumari S. [c]

[a] *Mar Baselious College of Engineering and Technology, Trivandrum, India*
[b] *Centre for Development of Advanced Computing (C-DAC), Trivandrum, India*
[c] *College of Engineering Trivandrum, Kerala, India*

Received 27 September 2014; received in revised form 3 August 2016; accepted 6 October 2016

Abstract

An electric propulsion system is generally based on torque controlled electric drive and DC series motors are traditionally used for propulsion system. Induction machines, which are reliable, low cost and have less maintenance, satisfy the characteristics of the propulsion and reinstating the DC series motor. Field oriented control (FOC) of induction machines can decouple its torque control from field control which allows the induction motor to act like a separately excited DC motor. In this paper, the characteristic control of induction motor is achieved through appropriate design modification of induction motor by varying magnetizing current to produce maximum torque in field weakening (FW) region. Thus to improve the torque capability of induction machine in FW region by varying machine parameters. The sensorless operation of the induction motor is carried out by adopting model reference adaptive system (MRAS) using sliding mode control (SMC) and a FW algorithm based on the voltage and current constraints. The simulation of the induction motor drive models based on the design options have been carried out and analyzed the simulation results.

Keywords: Field weakening; Induction machine; Model reference adaptive system; Sliding mode observer

1. Introduction

Propulsion system used in applications like electric vehicle, rolling stock and industrial floor material movement etc., requires high torque at low speeds for starting and climbing and nearly constant power at high speeds. The characteristic for propulsion is achieved in DC series motor through construction and applying variable DC voltage. When compared to DC motor, induction motor is rugged, reliable, lighter, low cost, and has less maintenance requirement. These features

* Corresponding author.
E-mail address: nishacharu@gmail.com (N. G.K.).
Peer review under the responsibility of Electronics Research Institute (ERI).

Production and hosting by Elsevier

http://dx.doi.org/10.1016/j.jesit.2016.10.002

make induction motor an ideal candidate for propulsion, even in applications that demand a fast dynamic response. Recent advancement in power electronics, microprocessor revolution and several new control technologies, such as vector and direct torque controls made it possible to replace DC machines with induction motors in applications like propulsion (Emadi et al., 2008).

The torque and speed in DC motor can be controlled independently by controlling armature current and field current respectively which ensures that DC motor has good dynamic performance. A speed adaptive flux observer with an adaptive compensator for the variation of the rotor resistance was proposed in Kubota and Nakano (1993). Based on the model reference adaptive control theory, a speed estimator with pole placement in Gadoue et al. (2010) was developed. Speed estimation by the output difference of the current model and voltage model was proposed in Jotten and Maeder (1983). A speed and position estimator based on the introduction of a constant-frequency carrier signal in the stator currents was developed in Dixon and Rivarola (1996). A novel estimation strategy for the very-low-speed operation to estimate both the instantaneous speed and load disturbance torque using Kalman filter was proposed in Kim and Sul (1996). In a sensorless drive, the speed could be accurately estimated through some sophisticated observer. A novel model reference adaptive system type rotor speed estimator for the vector-controlled IM drive was designed in Orlowska-Kowalska and Dybkowski (2010). Several observers are available: full order observers (Yamamoto et al., 2004), methods based on the Extended Kalman Filter (Bolognani et al., 1999). State estimation can also be done using sliding mode observers (Utkin, 1993) for the IM.

In propulsion purpose, the induction motor has to operate at speeds higher than the rated one, which is achieved by field (flux) weakening. During the past two decades, several research papers were presented in order to achieve the maximum torque capability of the machine in the FW region and suggested various approaches (Kim and Sul, 1995). Constant power operation at high speeds is achieved through field weakening. The constant power region of operation is very useful in traction, electric vehicles, and machine-tool spindle drives. Torque control in field weakening region using FOC has been investigated in Abu Rub et al. (2012).

The FW approaches can be categorized as: (i) variation of stator flux in inverse proportion to the rotor speed ($1/\omega_r$); (ii) feed forward reference flux generation on machine equations or machine models and (iii) closed loop control of the stator voltage or voltage detection model. The first approach as presented in Shin et al. (2002), which is the most frequently used one in FW control, the flux is established inversely proportional to the motor speed. The method cannot produce maximum output torque for the available current nor the full utilization of DC-link voltage. The second approach, as presented in Bunte et al. (1996), relies on the nonlinear equations of machine model and the constraints of voltage and current, which makes it parameter dependent. Thus the method can provide accurate results only if magnetic saturation is considered with known machine parameters of sufficient accuracy. The third approach as described in Lin and Lai (2011), maximum available inverter voltage is utilized to produce maximum torque in FW region when the excitation level is adjusted by closed loop control of the machine voltage.

In most of the approaches, maximum available inverter voltage is utilized to produce maximum torque in FW region when the excitation level is adjusted by closed loop control of the machine voltage. Field weakening has to be done without violating either current limit or voltage limit in such a manner that accelerating torque follows maximum torque trajectory. Most commonly used methods of excitation control do not fully utilize the installed inverter power which causes a reduction of torque and power down to 65%. Alternative methods are needed to produce the maximum torque that the induction motor could possibly develop at FW region.

In this paper, a control strategy is developed for SVM inverter fed induction motor based on sensorless FOC scheme in FW region. A novel idea is proposed to improve the torque capability in FW region by design modification of the induction motor. The torque-speed characteristics of various design options are evaluated and compared by generating simulation results by using MATLAB/Simulink. The paper is organized as follows: In the first section, the mathematical model and FOC of induction motor are reviewed. In the next sections, implementation of SVM inverter with FOC in sensorless operation and the FW control of induction machine are presented. Then, the design modification and design options for induction motor are proposed. Thus to improve the torque capability of induction machine in FW region by varying machine parameters. Finally, simulation results for evaluating the performance of the various design options and discussions are presented.

Please cite this article in press as: G.K., N., et al., Torque capability improvement of sensorless FOC induction machine in field weakening for propulsion purposes. J. Electr. Syst. Inform. Technol. (2016), http://dx.doi.org/10.1016/j.jesit.2016.10.002

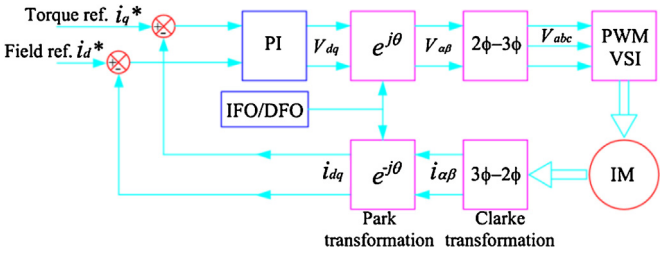

Fig. 1. Field oriented controlled induction motor drive system.

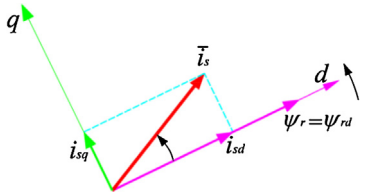

Fig. 2. Field orientation in d–q reference frame.

2. Field oriented control of induction machine

Space vector method can be used as a mathematical tool for the analysis of the electric machines and the complete set of equations can be expressed in the stationary coordinate α–β system as (Lakaparampil et al., 1996):

$$\vec{V}_{s\alpha}(t) = R_s \vec{i}_{s\alpha} + \frac{d\vec{\psi}_{s\alpha}}{dt} \tag{1}$$

$$\vec{V}_{s\beta}(t) = R_s \vec{i}_{s\beta} + \frac{d\psi_{s\beta}}{dt} \tag{2}$$

$$0 = R_r \vec{i}_{r\alpha} + \frac{d\psi_{r\alpha}}{dt} + \omega_r \vec{\psi}_{r\beta} \tag{3}$$

$$0 = R_r \vec{i}_{r\beta} + \frac{d\psi_{r\beta}}{dt} - \omega_r \vec{\psi}_{r\alpha} \tag{4}$$

The machine torque, T_d, can be expressed from the stator flux linkage and the stator current as:

$$T_d = \frac{2}{3}\frac{P}{2}\frac{L_m}{L_r}\left(\psi_{s\alpha} i_{s\beta} - \psi_{s\beta} i_{s\alpha}\right) \tag{5}$$

R_s—stator resistance, R_r—rotor resistance, T_d—electromagnetic torque, ω—angular speed, p—number of poles, τ_r—rotor time constant, i_{mr}—rotor magnetizing current, ω_{slip}—slip speed, ω_e—rotor flux speed, σ_r—rotor leakage factor.

Field oriented control of induction machine can decouple its torque control from field control to give dynamic performance comparable to the separately excited DC motor. Independent control of motor flux and torque can be obtained by this method and possible by connecting coordinate system with rotor flux vector (Leonhard, 1996). Figs. 1 and 2 show the block diagram of field oriented controlled induction motor drive system and d–q reference frame. Generally FOC is used for improving the dynamic performance of induction motor drives for propulsion. FOC implies the transition of coordinates from the stationary reference stator frame to rotating reference rotor frame (Nisha et al., 2012a).

By applying the rotor flux-oriented control the rotor flux linkage exists on the d-axis only, thus the rotor flux linkage can be adjusted by controlling the d-axis stator current and thus the field orientation concept in rotating reference frame can be written as:

$$\psi_{rd} = \psi_r = L_m\left(1 + \sigma_r\right) i_{rd} + L_m i_{sd} = L_m i_{mr} \tag{6}$$

Please cite this article in press as: G.K., N., et al., Torque capability improvement of sensorless FOC induction machine in field weakening for propulsion purposes. J. Electr. Syst. Inform. Technol. (2016), http://dx.doi.org/10.1016/j.jesit.2016.10.002

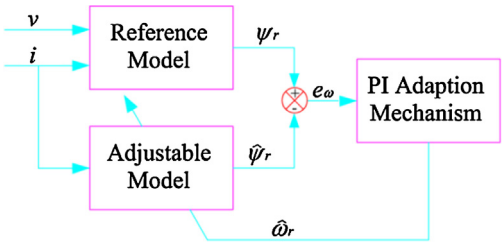

Fig. 3. Bock diagram of MRAS-SM speed estimator.

In induction motor mechanical speed is defined as the difference between rotor flux speed and slip angular frequency:

$$\omega_r = \omega_e - \omega_{slip} \tag{7}$$

$$\frac{d}{dt}\psi_{rq} + (\omega_e - \omega_r)\,\psi_{rd} + R_r i_{rq} = 0 \tag{8}$$

The machine torque can be controlled by regulating the q-axis stator current and can be expressed in terms of load torque as:

$$J\frac{d\omega_r}{dt} = \frac{2}{3}\frac{P}{2}\frac{L_m}{(1+\sigma_r)} i_{mr} i_{sq} - T_L \tag{9}$$

3. Sensorless operation of induction motor based on MRAS-sliding mode control

Sensorless control of induction machine is now attracting wide attention, both in the field of electrical drives and in the field of dynamic control. One of the most popular classes of observers is MRAS. This scheme computes a desired state called as the functional candidate using two different models. In the rotor flux based MRAS the rotor flux is used as an output value for the model to estimate the rotor speed. They are obtained in the stationary reference frame are referred to as voltage model and current model respectively (Nisha et al., 2013a). The adaptive scheme for the MRAS estimator is designed based on Popov's criteria for hyper stability concept, this relate to the stability properties of a class of feedback systems. This will result in a stable and quick response system where the convergence of the estimated value to the actual value can be assured with suitable dynamic characteristics. Popov's criterion of hyper-stability for a globally asymptotically stable system is used in deriving the speed estimation relation (Nisha et al., 2013b). Fig. 3 shows block diagram of MRAS speed estimator.

The reference value of the rotor flux components in the stationary frame are generated from the monitored stator voltage and current components given as:

$$\begin{bmatrix} \dot{\psi}_{r\alpha} \\ \dot{\psi}_{r\beta} \end{bmatrix} = \frac{L_r}{L_m}\begin{bmatrix} V_{s\alpha} \\ V_{s\beta} \end{bmatrix} - \begin{bmatrix} R_s + \sigma L_s p & 0 \\ 0 & R_s + \sigma L_s p \end{bmatrix}\begin{bmatrix} i_{s\alpha} \\ i_{s\beta} \end{bmatrix} \tag{10}$$

The adaptive model contains the estimated rotor speed, which represents the rotor equation and is usually known as the current model. The adaptive values of rotor flux components are given as:

$$\begin{bmatrix} \dot{\hat{\psi}}_{r\alpha} \\ \dot{\hat{\psi}}_{r\beta} \end{bmatrix} = \frac{L_m}{\tau_r}\begin{bmatrix} i_{s\alpha} \\ i_{s\beta} \end{bmatrix} + \begin{bmatrix} -\frac{1}{\tau_r} & -\hat{\omega}_r \\ \hat{\omega}_r & -\frac{1}{\tau_r} \end{bmatrix}\begin{bmatrix} \hat{\psi}_{r\alpha} \\ \hat{\psi}_{r\beta} \end{bmatrix} \tag{11}$$

The error e_ω between calculated and estimated state variables is then used to drive an adaption mechanism which generates the estimated speed. Fig. 4 shows MRAS representation as a non linear feedback system. The tuning signal, e_ω actuates the rotor speed and can be represented as:

$$e_\omega = \psi_{r\beta}\hat{\psi}_{r\alpha} - \psi_{r\alpha}\hat{\psi}_{r\beta} \tag{12}$$

Please cite this article in press as: G.K., N., et al., Torque capability improvement of sensorless FOC induction machine in field weakening for propulsion purposes. J. Electr. Syst. Inform. Technol. (2016), http://dx.doi.org/10.1016/j.jesit.2016.10.002

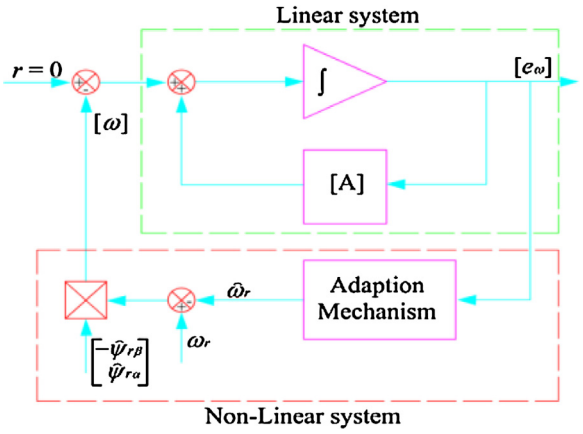

Fig. 4. MRAS representation as a non-linear feedback system.

SMC is one of the effective non linear robust control approaches since it provides system dynamics with an invariant property to uncertainties once the system dynamics are controlled in the sliding mode. Sliding mode control is a control strategy in variable structure system (VSS) in which a control law is designed so as to bring the system trajectory on the sliding surface. The sliding mode control should be chosen such that the candidate Lyapunov function, V which is a scalar function of S and its derivative satisfies the Lyapunov stability criteria as:

$$\dot{V}(S) = S(x)\dot{S}(x) \tag{13}$$

The control rule is written as:

$$u(t) = u_{eq}(t) + u_{sw}(t) \tag{14}$$

where, $u(t)$ is the control vector, $u_{eq}(t)$ is the equivalent control vector and $u_{sw}(t)$ is the switching vector and must be calculated so that stability condition for the selected control is satisfied.

$$u_{sw}(t) = \eta sign(S(x,t)) \tag{15}$$

$$\text{sign}(S) = \begin{cases} -1 & for \quad S < 0 \\ = 0 & for \quad S = 0 \\ +1 & for \quad S > 0 \end{cases}$$

The switching control depends on the sign of the switching surface and η is the hitting control gain which makes (13) negative definite, whose main purpose is to make the sliding condition viable and the value of η should be large enough to overcome the effect of external disturbance. This is attained when:

$$\hat{\omega}_r = u_{eq} + u_{sw} \tag{16}$$

The drastic change of input is avoided by introducing a boundary layer with width, ϕ. By replacing $sign(s)$ with $sat(S/\phi)$, then (15) becomes:

$$u_{sw} = \eta sat(S/\phi) \tag{17}$$

$$sat(S/\phi) = \begin{cases} sign(S/\phi) & if\,|\,(S/\phi)\,| \geq 1 \\ (S/\phi) & if\,|\,(S/\phi)\,| < 1 \end{cases} \tag{18}$$

A natural solution to reduce the chattering in the estimated speed is by means of a Low-Pass Filter (LPF):

$$u_{sw}{}' = \frac{1}{\mu s + 1} u_{sw} \tag{19}$$

Please cite this article in press as: G.K., N., et al., Torque capability improvement of sensorless FOC induction machine in field weakening for propulsion purposes. J. Electr. Syst. Inform. Technol. (2016), http://dx.doi.org/10.1016/j.jesit.2016.10.002

4. Field weakening control of induction motor

The field oriented control principle on AC motor take the advantages of transforming the variables from the physical three phase a–b–c system to a stationary coordinate α–β or rotating reference frame d–q. In a separately excited DC motor the excitation flux is controlled by varying the DC current through the field winding (Nisha et al., 2013d). In order to increase the speed above the rated speed, the flux must be decreased or weakened while the voltage is kept constant at rated value (Seung-Ki Sul, 2011). The induction motor operation can be divided into three speed ranges, (i) constant electromagnetic torque region or base speed region, (ii) constant power speed region (FW-I) and (iii) constant slip frequency region (FW-II).

In FW, due to slow variations of flux linkage and current, terms due to flux variation, current variations in the stator voltage equations and the voltage drop due to the stator resistance can be neglected in FW region. To achieve better overload capability of a controlled drive and to improve its dynamic performance, the maximum stator current is usually set to a higher value than the rated machine current. The current vector is restricted to remain within in a circle of diameter I_{sm}. The maximum current to the machine is also limited and the current limit boundary is a circle, whose radius depends only on the current rating I_{sm}. The current constraint of the inverter can be expressed as follows,

$$I_{sd}{}^2 + I_{sq}{}^2 \leq I_{\mathrm{sm}}{}^2 \tag{20}$$

The maximum phase voltage is decided by the PWM strategy and the available DC bus voltage. Space vector modulation is a sophisticated PWM method that provides advantages such as higher DC bus voltage utilization and lower total harmonic distortion (Holmes and Lipo, 2003; Nisha et al., 2012e,c,d,b). If the magnitude of the voltage reference vector is lower than $V_{DC}/\sqrt{3}$, the space-vector modulator produces sinusoidal output voltages, the voltage limit ellipse equation as follows:

$$V_{sd}{}^2 + V_{sq}{}^2 \leq V_{\mathrm{sm}}{}^2 \tag{21}$$

The base speed in which the field weakening begins, is decided by the voltage and current constraints as:

$$\omega_b = \frac{V_{sm}}{L_s}\sqrt{\frac{1}{[\sigma^2(I_{sm}{}^2 - i_{sd}{}^2) + i_{sd}{}^2]}} \tag{22}$$

In constant torque region, the output current of the inverter is equal to the limit value to prevent the magnetic saturation of the induction machine, the output voltage is lower than the limit value and the rotor speed is less than the rated speed. In constant power speed range as the output voltage and the output current of the inverter are equal to the limit values, the speed increases beyond the base speed, the size of ellipse decreases and this region ends, above which there is no more intersection point between the ellipse and circle. In constant slip frequency region (decreasing power speed range) the voltage applied to the motor equal to the limit value and the motor current is lower than the limit value due to the high back emf which prevents the inverter from injecting the maximum current into the motor.

5. Design modification of induction motor

Existing constraints for the operation at field weakening are the maximum output voltage and the permitted maximum current of the inverter. To produce the maximum torque that the machine could possibly develop, the excitation level of field weakening must be appropriately adjusted. Most commonly used methods of excitation control do not fully utilize the installed inverter power which can lead to a reduction of torque and power down to 65%. The innovative approach proposed in this paper is to carry out appropriate design modification of the induction motor by varying the rated value of power factor so as to explore maximum torque and power compared to its rated values. The main specifications for the design of a three phase squirrel cage induction motor are: rated output power in HP or kW, frequency in Hz, voltage in volts, speed in rpm, efficiency, power factor and full load current in ampere. The stator and rotor dimensions are determined by independent variables which are: stator slot height, stator tooth width, rotor slot height, rotor tooth width, air-gap length, air gap flux density, stack length, outer stator diameter, stator wire size and electrical steel type. Besides the above independent variables, the design involves some non-linear constraints which concern mainly the motor performances.

Please cite this article in press as: G.K., N., et al., Torque capability improvement of sensorless FOC induction machine in field weakening for propulsion purposes. J. Electr. Syst. Inform. Technol. (2016), http://dx.doi.org/10.1016/j.jesit.2016.10.002

Table 1
Machine parameters of design options for Case-1 (for 10 kW).

Parameters		Design options				Unit
		A	B	C	D	
Full load output	P	10.0	10.0	10.0	10.0	kW
Line voltage	V	220	220	220	220	V
Full load current	I_L	32.4	36.4	41.6	48.6	A
Synchronous	N_s	1500	1500	1500	1500	rpm
Rated torque	T_d	65	65	65	65	N-m
Frequency	f	50	50	50	50	Hz
No. of poles	$Pole$	4	4	4	4	
Power factor	pf	0.9	0.8	0.7	0.6	
Efficiency	η	89.4	88.5	87.6	86.1	%
Stator bore	D	185	190	200	210	mm
Core length	L	145	150	155	165	mm
Air gap length	l_g	0.53	0.54	0.55	0.57	mm
Diameter of conductors		1.80	1.90	2.06	2.12	mm
No. of turns/phase	T_s	112	106	96	86	Nos.
Diameter of rotor	D_r	184	189	199	209	mm
Area of rotor bar	A_{br}	57	54	54	45	mm^2
Magnetizing current	i_{mr}	24.3	28.9	33.7	41.5	A

Table 2
Machine parameters of design options for Case-2 (for 30 kW).

Parameters		Design options				Unit
		A	B	C	D	
Full load output	P	30.0	30.0	30.0	30.0	kW
Line voltage	V	220	220	220	220	V
Full load current	I_L	97.1	109.3	124.9	145.7	A
Synchronous speed	N_s	1500	1500	1500	1500	rpm
Rated torque	T_d	195	195	195	195	N-m
Frequency	f	50	50	50	50	Hz
No. of poles	$Pole$	4	4	4	4	
Power factor	pf	0.9	0.8	0.7	0.6	
Efficiency	η	91.9	91.3	90.4	89.4	%
Stator bore	D	260	270	280	295	mm
Core length	L	205	210	220	230	mm
Air gap length	l_g	0.66	0.68	0.70	0.72	mm
Diameter of conductors		2.67	2.84	3.03	3.27	mm
No. of turns/phase	T_s	56	52	48	44	Nos.
Diameter of rotor	D_r	259	269	279	294	mm
Area of rotor bar	A_{br}	85	79	73	67	mm^2
Magnetizing current	i_{mr}	56.8	63.2	64.5	66.9	A

Based on the standard design procedure, design spread sheets are developed for three phase squirrel cage induction machine. Design models are done for two cases namely, Case-1 and Case-2, for 10 kW and 30 kW respectively. Design modifications are adopted for various options to modify torque speed characteristics to meet propulsion application. Design options are generated by reducing the power factor and the options are named as Design-A, Design-B, Design-C and Design-D for power factors equal to 0.9, 0.8, 0.7 and 0.6 respectively. The design values obtained from the design sheet for the above design options are tabulated and presented in Tables 1 and 2 for Cases-1 and 2 respectively.

Please cite this article in press as: G.K., N., et al., Torque capability improvement of sensorless FOC induction machine in field weakening for propulsion purposes. J. Electr. Syst. Inform. Technol. (2016), http://dx.doi.org/10.1016/j.jesit.2016.10.002

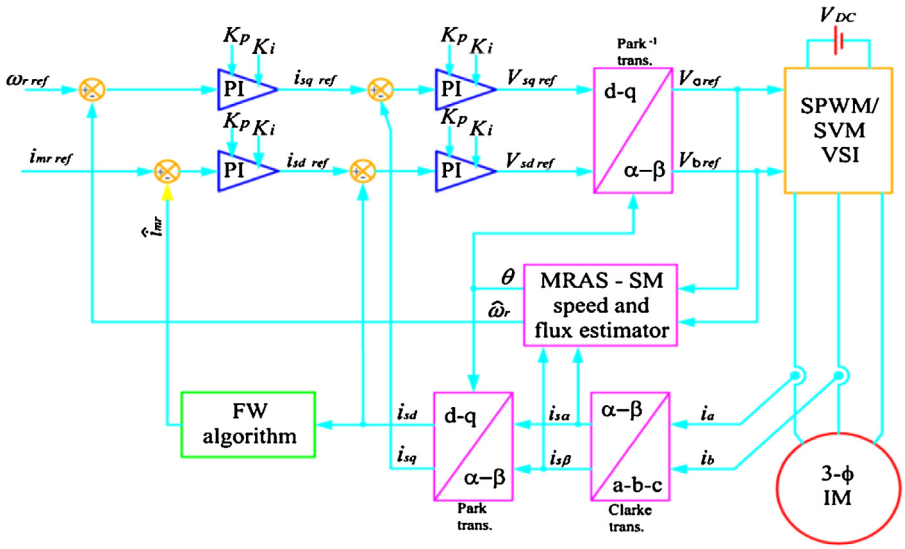

Fig. 5. Block diagram of sensorless FOC induction machine using MRAS-SM speed estimator in FW region.

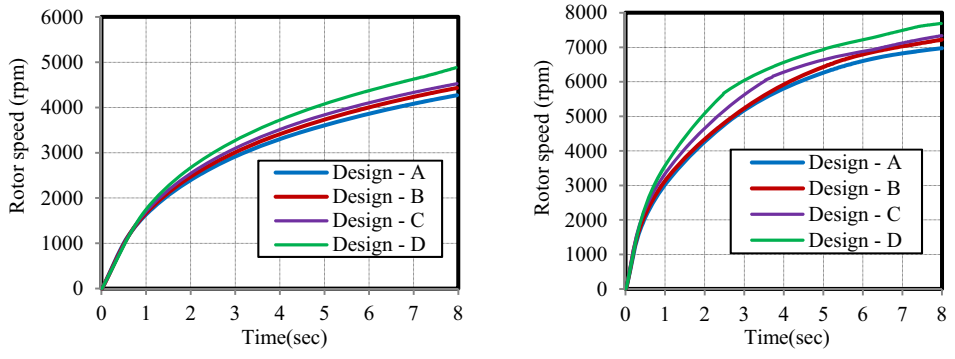

(a) case-1 (for 10 kW) (b) case-2 (for 30 kW)

Fig. 6. Rotor speed vs. time.

6. Simulation results and discussion

The Simulink/MATLAB model for FOC induction machine with sensor using SVM inverter is developed in Nisha et al. (2013c). The above model is extended from base speed region to FW region in Nisha et al. (2014a,b). Fig. 5 illustrates the simulation model for sensorless FOC induction machine using MRAS-SM speed estimator in FW region. For comparing the performance of the design options, Design-A, Design-B, Design-C and Design-D, simulations are carried out for these design options using the above model. In the simulation, the motor starts from a standstill state in no load condition and the speed responses are shown in Fig. 6. From the results, it is clear that the rotor speed increases from Design-A to Design-D, which means the rotor speed increases with the reduction in power factor. The maximum attainable speed at 8 s after starting the machine, is increased from Design-A to Design-D in both cases as given in Table 3.

Fig. 7 shows the variation of electromagnetic torque (p.u.) with respect to rotor speed (p.u.) for various design options. Torque capability is improved in the FW region when the power factor decreases as demonstrated in Fig. 7 and Table 4.

Variation of power (p.u.) with respect to rotor speed (p.u.) is presented in Fig. 8 for the design options. In the constant power region of the FW range, power increases from Design-A to Design-D, which implies that power increases with

Please cite this article in press as: G.K., N., et al., Torque capability improvement of sensorless FOC induction machine in field weakening for propulsion purposes. J. Electr. Syst. Inform. Technol. (2016), http://dx.doi.org/10.1016/j.jesit.2016.10.002

Table 3
Speed response at 8 s.

Design options	ω_r (rpm)	
	Case-1	Case-2
Design-A	4270	6973
Design-B	4430	7225
Design-C	4525	7335
Design-D	4885	7687

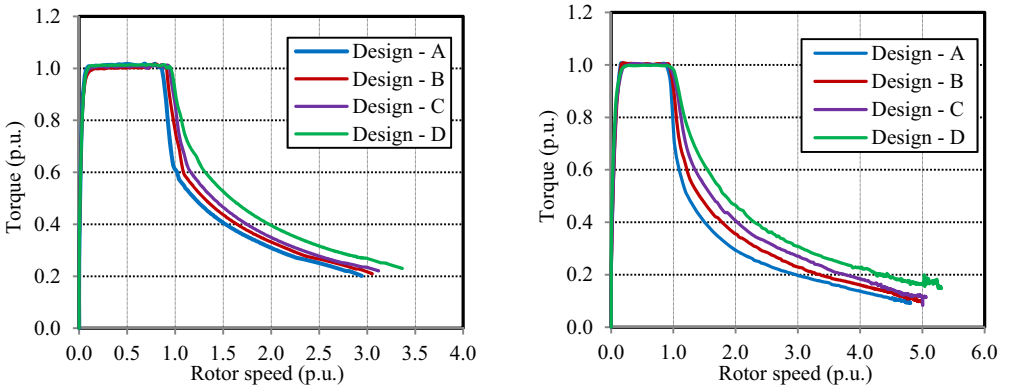

Fig. 7. Torque vs. rotor speed.

Table 4
Torque capability (p.u.).

Design options	$\omega_r = 2.0$ p.u.		$\omega_r = 3.0$ p.u.	
	Case-1	Case-2	Case-1	Case-2
Design-A	0.309	0.292	0.201	0.196
Design-B	0.331	0.353	0.217	0.229
Design-C	0.350	0.405	0.234	0.271
Design-D	0.395	0.464	0.268	0.307

Table 5
Maximum power (p.u.).

Design options	$\omega_r = 2.0$ p.u.		$\omega_r = 3.0$ p.u.	
	Case-1	Case-2	Case-1	Case-2
Design-A	0.618	0.580	0.603	0.588
Design-B	0.662	0.706	0.651	0.687
Design-C	0.700	0.810	0.702	0.813
Design-D	0.790	0.928	0.804	0.921

the reduction in power factor. Table 5 shows that increase of power for Design-D compared to Design-A is about 33% and 56% in Cases 1 and 2 respectively for rotor speed of 3.0 p.u.

The variation of rotor magnetizing current (p.u.) with respect to rotor speed (p.u.) is shown in Fig. 9. The magnetizing current curves for various design options are dissimilar in the entire speed range.

By observing the simulation results, it ensures that improvement of torque capability and power in FW region is possible by decreasing the power factor. As power factor decreases flux increases and torque improvement is obtained

Please cite this article in press as: G.K., N., et al., Torque capability improvement of sensorless FOC induction machine in field weakening for propulsion purposes. J. Electr. Syst. Inform. Technol. (2016), http://dx.doi.org/10.1016/j.jesit.2016.10.002

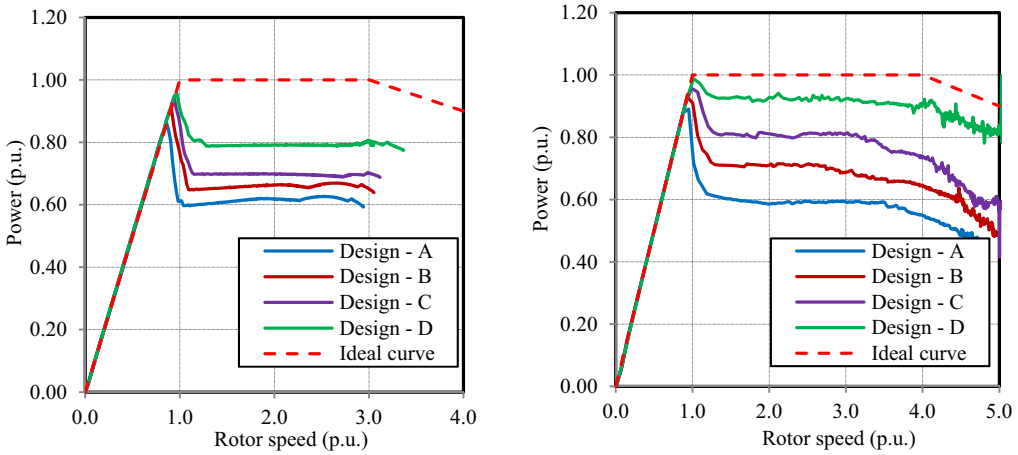

(a) case-1 (for 10 kW) (b) case-2 (for 30 kW)

Fig. 8. Power vs. rotor speed.

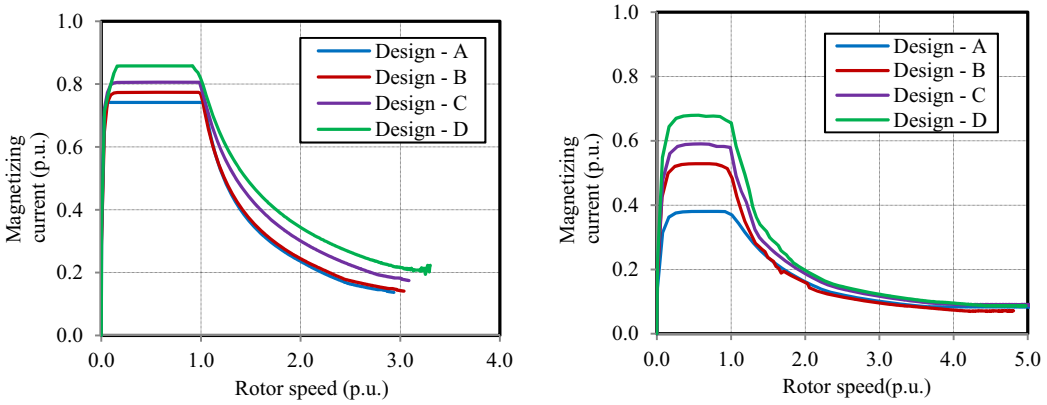

(a) case-1 (for 10 kW) (b) case-2 (for 30 kW)

Fig. 9. Magnetizing current vs. rotor speed.

for wide range of speed. It is also observed from the above simulation results that better results can be achieved when the power rating increases from 10 kW to 30 kW.

7. Conclusions

The original contribution in this paper is an innovative approach to improve the torque capability of induction machine in FW region by varying machine parameters rather than the conventional approach of maximizing the DC link voltage. MATLAB/Simulink simulation models for field oriented controlled induction machine without sensor using SVM inverter is used to operate various design options of induction machine for comparing the torque–speed characteristics. The maximum attainable rotor speed and torque capability of FOC induction machine in FW region are improved by decreasing the power factor of the induction machine from rated value. The maximum rotor speed attainable is increased when the power factor is reduced. Toque capability is improved by 33%–56% in FW region, when the power factor is reduced by 33%. Constant power in FW region is increased by 57% when the power factor is reduced by 33%. Here field weakening I & II is used to get wide range of speed. As power factor decreases flux increases and torque improvement is obtained for wide range of speed. In conventional normally two times the base speed can be obtained, but in propulsion wide range of speed as high as four times the speed can be attained. In future

Please cite this article in press as: G.K., N., et al., Torque capability improvement of sensorless FOC induction machine in field weakening for propulsion purposes. J. Electr. Syst. Inform. Technol. (2016), http://dx.doi.org/10.1016/j.jesit.2016.10.002

work, the robustness of the findings can be further investigated by hardware implementations and by generating the experimental results for ensuring the effectiveness of the proposed approach.

Acknowledgment

The first author acknowledges support from SPEED-IT Research Fellowship from IT Department of the Government of Kerala, India.

References

Abu Rub, H., Iqbal, Atif, Guzinski, Jaroslaw, 2012. High Performance Control of AC Drives. Wiley, New York, pp. 375–388.
Bolognani, S., Oboe, R., Zigliotto, M., 1999. Sensorless full digital PMSM drive with EKF estimator of speed and rotor position. IEEE Trans. Ind. Electron. 46 (February), 184–191.
Bunte, A., Grotstollen, H., Krafka, P., 1996. Field weakening of induction motors in a very wide region with regard to parameter uncertainties. In: Proceedings of the IEEE Power Electronics Specialists Conference, PESC, June, pp. 944–950.
Dixon, J.W., Rivarola, J.N., 1996. Induction motor speed estimator and synchronous motor position estimator based on a fixed carrier frequency signal. IEEE Trans. Ind. Electron. 43 (August), 505–509.
Emadi, A., Lee, Y.J., Rajashekara, K., 2008. Power electronics and motor drives in electric, hybrid electric and plug-in hybrid electric vehicles. IEEE Trans. Ind. Electron. 55 (6), 2237–2245.
Gadoue, S.M., Giaouris, D., Finch, J.W., 2010. MRAS sensorless vector control of an induction motor using new sliding mode and fuzzy logic adaption mechanisms. IEEE Trans. Energy Convers. 25 (June (2)), 394–402.
Holmes, D.G., Lipo, T.A., 2003. Pulse Width Modulation for Power Converters: Principles and Practice. Wiley IEEE Press, New Jersey.
Jotten, R., Maeder, G., 1983. Control method for good dynamic performance induction motor drives based on current and voltage as measured quantities. IEEE Trans. Ind. Appl. 19 (May/June (3)), 356–363.
Kim, S.H., Sul, S.K., 1995. Maximum torque control of an induction machine in the field weakening region. IEEE Trans. Ind. Appl. 31 (July/August (4)), 787–794.
Kim, H.W., Sul, S.K., 1996. A new motor speed estimator using Kalman filter in low-speed range. IEEE Trans. Ind. Electron. 43 (August), 498–504.
Kubota, K.M.H., Nakano, T., 1993. DSP-based speed adaptive flux observer of induction motor. IEEE Trans. Ind. Appl. 29 (March/April), 344–348.
Leonhard, W., 1996. Control of Electrical Drives. Springer, New York, pp. 163–180.
Lin, P.Y., Lai, Y.S., 2011. Novel voltage trajectory control for field-weakening operation of induction motor drives. IEEE Trans. Ind. Appl. 47 (January/February (1)), 122–127.
Lakaparampil, Z.V., Fathima, K.A., Ranganathan, V.T., 1996. Design modeling simulation and implementation of vector controlled induction motor drive. January In: Proceedings of the PEDES, 2, pp. 862–868.
Nisha, G.K., Lakaparampil, Z.V., Ushakumari, S., 2012a. Sensorless vector control of SVPWM fed induction machine using MRAS-sliding mode. In: Proceedings of IEEE International Conference on Green Technology, ICGT, 2012, December, pp. 29–36.
Nisha, G.K., Ushakumari, S., Lakaparampil, Z.V., 2012b. Online harmonic elimination of SVPWM for three phase inverter and a systematic method for practical implementation. IAENG Int. J. Comput. Sci. 39 (May (2)), 220–230.
Nisha, G.K., Ushakumari, S., Lakaparampil, Z.V., 2012. Harmonic elimination of space vector modulated three phase inverter. Lecture Notes in Engineering and Computer Science: Proceedings of the International Multi-conference of Engineers and Computer Scientists, March 2012, pp. 1109–1115.
Nisha, G.K., Ushakumari, S., Lakaparampil, Z.V., 2012d. CFT based optimal PWM strategy for three phase inverter. In: Proceedings of IEEE International Conference on Power, Control and Embedded Systems, ICPCES, 2012, December, pp. 1–6.
Nisha, G.K., Ushakumari, S., Lakaparampil, Z.V., 2012e. Method to eliminate harmonics in PWM: a study for single phase and three phase. In: Proceedings of International Conference on Emerging Technology Trends on Advanced Engineering Research, ICETT 2012, Kollam, India, February, pp. 598–604.
Nisha, G.K., Lakaparampil, Z.V., Ushakumari, S., 2013. Sensorless field oriented control of SVM inverter fed Induction machine in field weakening region using sliding mode observer. Lecture Notes in Engineering and Computer Science: Proceedings of the 7th World Congress on Engineering, London, July 2013, pp. 1174–1181.
Nisha, G.K., Lakaparampil, Z.V., Ushakumari, S., 2013b. Performance study of field oriented controlled induction machine in field weakening using SPWM and SVM fed inverters. Int. Rev. Model. Simul. 6 (June (3)), 741–752.
Nisha, G.K., Lakaparampil, Z.V., Ushakumari, S., 2013c. FFT analysis for field oriented control of SPWM and SVPWM inverter fed induction machine with and without sensor. Int. J. Adv. Electr. Eng. 2 (June (4)), 151–160.
Nisha, G.K., Lakaparampil, Z.V., Ushakumari, S., 2013d. Four quadrant operation of sensorless FOC induction machine in field weakening region using MRAS-sliding mode observer. In: Proceedings of IEEE International Conference on Control Communication and Computing, ICCC, Trivandrum, India, December, pp. 33–38.
Nisha, G.K., Lakaparampil, Z.V., Ushakumari, S., 2014a. Effect of leakage inductance on torque capability of field oriented controlled induction machine in field weakening region. In: International Conference on Advances in Engineering and Technology, ICAET, March, pp. 741–752.
Nisha, G.K., Lakaparampil, Z.V., Ushakumari, S., 2014b. Four quadrant operation of field weakened FOC induction motor drive using sliding mode observer. In: Transactions on Engineering Technologies. Springer Publication, pp. 385–402, Special Volume of WCE, May 2014.

Please cite this article in press as: G.K., N., et al., Torque capability improvement of sensorless FOC induction machine in field weakening for propulsion purposes. J. Electr. Syst. Inform. Technol. (2016), http://dx.doi.org/10.1016/j.jesit.2016.10.002

Orlowska-Kowalska, T., Dybkowski, M., 2010. Stator-current-based MRAS estimator for a wide range speed sensorless induction-motor drive. IEEE Trans. Ind. Electron. 57 (April (4)), 1296–1308.

Seung-Ki Sul, 2011. Control of Electric Machine Drive Systems. Wiley, New Jersey, pp. 255–267.

Shin, M.H., Hyun, D.S., Cho, S.B., 2002. Maximum torque control of stator flux oriented induction machine drive in the field weakening region. IEEE Trans. Ind. Appl. 1 (January/February), 117–122.

Utkin, V.I., 1993. Sliding mode control design principles and applications to electric drives. IEEE Trans. Ind. Electron. 40 (February (1)), 23–36.

Yamamoto, Y., Yoshida, Y., Ashikaga, T., 2004. Sensorless control of PM motor using full order flux observer. IEEE Trans. Ind. Appl. 124 (August), 743–749.

Please cite this article in press as: G.K., N., et al., Torque capability improvement of sensorless FOC induction machine in field weakening for propulsion purposes. J. Electr. Syst. Inform. Technol. (2016), http://dx.doi.org/10.1016/j.jesit.2016.10.002